Macromolecular Research, Vol. 16, No. 8, pp 725-733 (2008)

Polyimide Multilayer Thin Films Prepared via Spin Coating from Poly(amic acid) and Poly(amic acid) Ammonium Salt

Youri Ha, Myeon-Cheon Choi, Namju Jo*, Il Kim, and Chang-Sik Ha*

Department of Polymer Science and Engineering, Pusan National University, Busan 609-735, Korea

Donghee Han and Sewon Han

Advanced Materials and Application Research Lab., Korea Electrotechnology Research Institute, P.O.Box 20, Changwon 641-600, Korea

Mijeong Han

Advanced Materials Division, Korea Research Institute of Chemical Technology, Daejeon 305-600, Korea

Received August 6, 2008; Revised October 21, 2008; Accepted November 3, 2008

Abstract: Polyimide (PI) multilayer thin films were prepared by spin-coating from a poly(amic acid) (PAA) and poly(amic acid) ammonium salt (PAAS). PI was prepared from pyromellitic dianhydride (PMDA) and 4,4'-oxydianiline (ODA) PAA. Different compositions of PAAS were prepared by incorporating triethylamine (TEA) into PMDA-ODA PAA in dimethylacetamide. PI multilayer thin films were spin-coated from PMDA-ODA PAA and PAAS. The PAAS comprising cationic and anionic moieties were spherical with a particle size of 20~40 nm. Some particles showed layers with ammonium salts, despite poor ordering. Too much salt obstructed the interaction between the polymer chains and caused phase separation. A small amount of salt did not affect the interactions of the interlayer structure but did interrupt the stacking between chains. Thermogravimetric analysis (TGA) showed that the average decomposition temperature of the thin films was 611 °C. All the films showed almost single-step, thermal decomposition behavior. The nanostructure of the multilayer thin films was confirmed by X-ray reflectivity (XRR). The LF 43 film, which was prepared with a 4:3 molar ratio of PMDA and ODA, was comprised of uniformly spherical PAAS particles that influenced the nanostructure of the interlayer by increasing the interaction forces. This result was supported by the atomic force microscopy (AFM) data. It was concluded that the relationship between the uniformity of the PAAS particle shapes and the interaction between the layers affected the optical and thermal properties of PI layered films.

Keywords: polyimide, multilayer films, spin coating, ammonium salt, nanostructure.

Introduction

Multilayer thin films have attracted considerable interest on account of their applications in a variety of areas, such as sensors, integrated optics, friction-reducing coatings, biological surfaces, light-emitting devices (LEDs), or surface-orientation layers.[1-5]

Aromatic polyimides (PIs) are well known high-performance polymeric materials owing to their excellent thermal stability and balanced mechanical and electrical properties.[6-10] These materials are finding many applications as adhesives, composites, fibers, films and electrical materials. These aromatic polyimides are suitable for preparing multilayer thin films. However, the polyimide multilayer system shows phase separation of each layer and a weak interaction between the layer interfaces. Various studies have added ion-containing organic materials to a polymer, such as metal salts[11,12] and organic salts, in an attempt to solve the problems. For example, attempts have been made to increase electron injection through the deposition of a very thin layer of a high polar material between a conjugated polymer and a cathode, such as inorganic salts, surface active agents and ion containing polymers of ionic groups randomly distributed in the non-polar backbone chains.[13,14] One important feature of these layers is that the thickness must be thin enough to allow carrier injection, usually tens of nanometers.

In this study, polyimide (PI) multilayer thin films with a

*Corresponding Authors. E-mails: csha@pusan.ac.kr or namjujo@pusan.ac.kr

strong interaction were prepared using ammonium salt. PI was prepared from pyromellitic dianhydride (PMDA) and 4,4′-oxydianiline (ODA). Poly(amic acid) ammonium salt (PAAS) with different compositions by incorporating triethylamine (TEA) into PMDA-ODA poly(amic acid) (PAA) in dimethylacetamide. This paper reports the nanostructure as well as the optical and thermal properties of PI multilayer thin films.

Experimental

Materials and Sample Preparation. Aromatic monomers, pyromellitic dianhydride (PMDA, 97%) and 4,4′-oxydianiline (ODA), were used to synthesize the precursor poly(amic acid) (PAA) of the polyimide. Poly(amic acid) salts (PAAS) was prepared by adding 3-triethylamine (TEA). All these materials were purchased from Aldrich (St. Louis, MO) and used as received. *N,N′*-dimethyl acetamide (DMAc) was distilled over calcium hydride under reduced pressure.

Synthesis of PMDA-ODA Poly(amic acid) (PAA). PMDA-ODA PAA was prepared as usual by reacting equimolar quantities of PMDA and ODA in DMAc under a nitrogen atmosphere at room temperature. The reaction was continued for 24 h to achieve a homogeneous mixture solution. After terminating the reaction, the solution was poured into an excess volume of toluene for precipitation. The precipitated solid, PMDA-ODA PAA, was filtered and washed several times with toluene to remove any remaining DMAc molecules. The final solid was dried under vacuum at 60 °C for 6 h. The solid was dissolved in 5 wt% DMAc.

Synthesis of PMDA-ODA PAA Salts (PAAS). As shown in Figure 1, PAAS was prepared from PAA in DMAc by incorporating TEA, followed by mixing to a homogeneous state. Three samples with different compositions were prepared (see Table I). In the first sample, a PMDA-ODA PAA solution was prepared with an equimolar ratio of PMDA and ODA in DMAc under a nitrogen atmosphere. The second sample was prepared with a 4:3 molar ratio of PMDA and ODA. The last sample was prepared from a 2:1 molar ratio of PMDA and ODA. Each reaction was continued for 16 h to produce a homogeneous mixture. The solid content of the solution was 5 wt%. After making the PAA solution, a given amount of TEA was added into the PAA solution at room temperature and the mixture was stirred for 45 min under a nitrogen atmosphere. Upon the addition of TEA, a large increase in viscosity was observed with local white precipitation of polymer, as reported by Kreuz *et al.*.[15] The

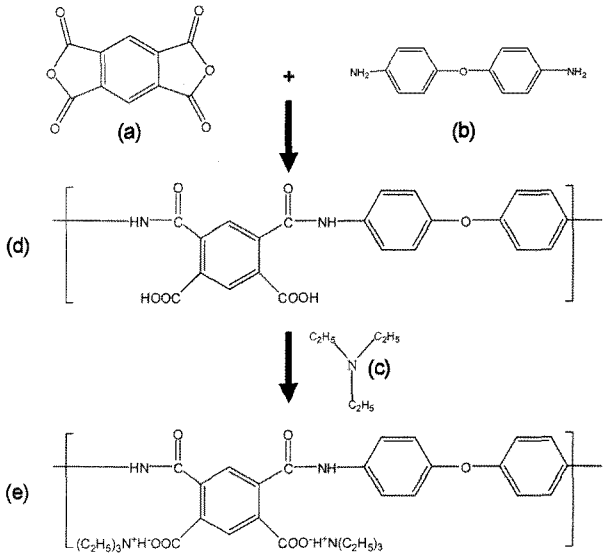

Figure 1. Chemical structures of (a) PMDA, (b) ODA, and (c) TEA with conversion from (d) PAA to (e) PAAS.

solution was poured into acetone, and the precipitated solid was filtered, dried under vacuum and pulverized in a mortar. Subsequent drying under vacuum at 40 °C for 24 h gave a light yellow PAAS powder.[15] The powder was dissolved in 5 wt% of DMAc.

Construction of PI Multilayer Thin Films Using a Spin Coating Method. Polyimide multilayer thin films were spin-coated from PAA and PAAS at 3,000 rpm. Briefly, 1 mL of PAA was placed onto a silicon wafer for 60 sec using a pipette. The substrate was then heated at 40 °C for 1 h. One milliliter of a PAAS solution was pipetted onto the substrate. The substrate was then heated at 40 °C for 1 h. PI multilayer thin films were easily fabricated by repeating the above 2 steps. After casting, the precursor films were kept at 40 °C for 12 h and then soft-baked at 80 °C for 6 h. The precursor films were then thermally imidized at 300 °C for 4 h to produce the polyimide multilayer thin films.

Measurements and Characterization. The functional groups of polyimide multilayer thin films were examined by Fourier transform infrared (FT-IR) spectroscopy (ATR mode, React IR™ 1000, Applied System, ASi). The materials were also characterized by ^{1}H nuclear magnetic resonance (NMR 300 MHz, DMSO, 293 K, Varian Unity Plus-300) spectroscopy. The particle diameter was measured using a Particle and Pore Size Analysis System (Korea Basic Science Institute, Particle Size Analyzer UPA-150, Microtrac). The sam-

Table I. Formulation of PAAS of Different Compositions (Molecular Weights were Measured by GPC.)

Sample Name	PMDA (molar ratio)	TEA (molar ratio)	ODA (molar ratio)	M_n	M_w	PDI
LF 11	1	2	1	5.08×10^5	8.93×10^5	1.75
LF 43	4	8	3	2.35×10^3	4.32×10^3	1.84
LF 21	2	4	1	9.70×10^2	1.50×10^3	1.54

ples for the dynamic light scattering (DLS) measurements were prepared as follows: the PAA precursor solutions were diluted with DMAc. The nanostructure of the polyimide multilayer thin films was examined by X-ray reflection (XRR). The XRR measurement was carried out at the Korea Basic Science Institute [Model: X'pert PRO MRD, CuK$_\alpha$ (λ=1.5418 Å)]. The thermal decomposition stability of the multilayer films was measured using a thermogravimetric analyzer (TGA Q50 Q Series, TA Instrument). The samples were heated to between 30 and 900 °C at a heating rate of 10 °C/min. The film thickness was measured using an Alpha-Step(ISIO, Kla-tencor Korea) at a scan speed of 10 μm/sec. The transparency of the PI multilayer thin films was measured by ultraviolet visible spectroscopy recorded on a HIT-MACHI U-2010 spectrometer that was optimized with a spectral width of 200-900 nm, a resolution of 0.5 nm, and a scanning rate of 200 nm/min. The molecular weights of the PAAS were measured using gel permeation chromatography (GPC) with a Waters 515 Differential Refractometer, Waters 410 HPLC Pump and two Styrogel HR 5E columns in DMF (0.1 mg/L) at 42 °C. The GPC was calibrated with polystyrene standards. The morphology of the PI multilayer thin films was confirmed by atomic force microscopy (AFM; Digital Instrument Nanoscope III). The cantilever used for the AFM measurements was V-shaped (VEECO). The bending spring constant of the cantilever was 0.022 N/m. The AFM measurements for polyimide multilayer thin films were prepared as follows: the precursor solutions were spin-coated onto Si wafers, which were cut into 5 mm × 5 mm square pieces, precleaned with acetone, and finally the dust was blown off prior to use. The subsequent soft-baking and thermal imidization processes were the same as described elsewhere.

Results and Discussion

Structure Analysis. Figure 2 shows the FT-IR spectra (ATR mode) of the PI multilayer thin films before and after imidization. The spectra of the multilayer thin films before imidization (Figure 2(a)) show the earmark absorption bands of the N-H and COOH groups around 3000 and 1600 cm^{-1}, respectively. After imidization (Figure 2(b)), the spectra show absorption bands (double peak) between 1780 and 1710 cm^{-1} corresponding to both symmetric and asymmetric C=O stretching of the imide group, respectively. The absorption bands around 1390-1380 and 730-710 cm^{-1} show the presence of the C-N stretching and an imide heterocyclic ring in the PAA/PAAS multilayer thin films. The band at 1168 cm^{-1} was assigned to the aromatic C_6H_4 or C_6H_2. In addition, in Figure 3(a), ^{1}H-NMR spectra confirmed the PAA and PAAS. The peaks at 1 and 3.5 ppm for TEA are related to two types of protons for -CH_3 and -CH_2- groups (Figure 3(a)). The ^{1}H NMR spectrum of PAA in Figure 3(b) shows four peaks at 6-9 ppm, which was assigned to benzene. The same peaks were confirmed for the PAAS (see Figure 3(c)). The two new peaks at 1 and 3 ppm were assigned to the protons for the attachment of TEA into PAA. The proton of -CH_2- of TEA were shielded by the proton of the COOH group of PAA, and that peak was shifted to the right. Another peak shown in Figure 3(c)-(e) indicates a COOH proton, which was shifted to the left due to deshielding of the N atom in TEA(see inset). The same trend was observed in the case of LF 43 and LF 21.

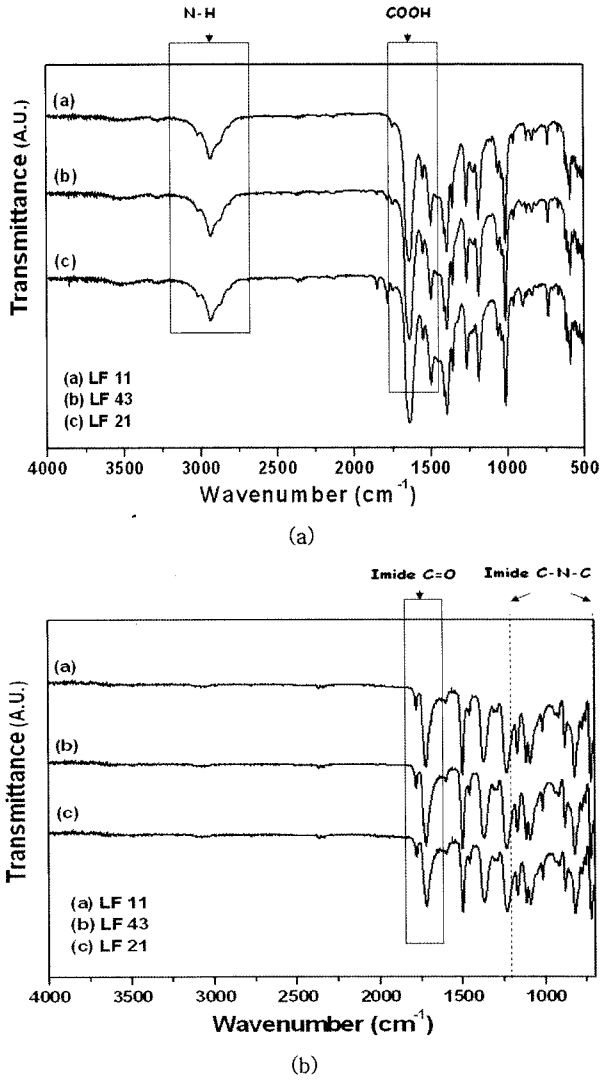

Figure 2. FT-IR spectra (ATR mode) of poly(amic acid) multilayer thin films (a) before and (b) after imidization.

In Table I, the GPC data show that the weight average molecular weights (M_w) of LF11, LF43 and LF21 were 8.93 × 10^5, 4.32 × 10^3 and 1.50 × 10^3, respectively. The molecular weight of these PAAS can be controlled by adjusting the degree of polymerization. The PAAS possessing cationic and anionic moieties were spherical (which will be shown later). Different amounts of PAAS can influence the inner structure of the polyimide multilayer thin films. It should be noted that

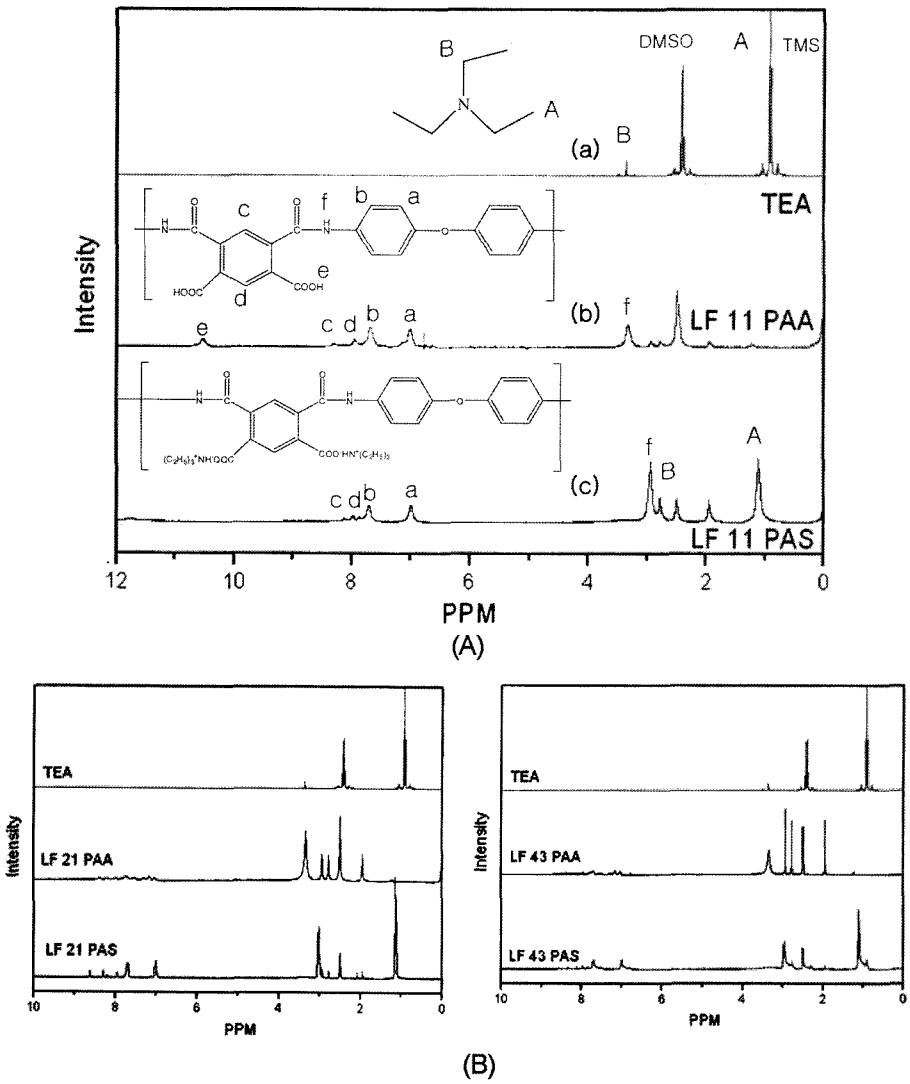

Figure 3. ^{1}H NMR spectra of A (LF11: (a) triethylamine (TEA), (b) poly(amic aicd)(PAA) and corresponding, (c) poly(amic acid) ammonium salt (PAS)) and B (LF43, LF21).

the three samples have low polydispersity (ranging from 1.54 to 1.84), indicating a narrow molecular weight distribution.

Surface Morphology and Dynamic Light Scattering. The AFM images of each layer show the domain structures. As shown in Figure 4 for 7 layers of LF11 multilayer thin films, the surface morphology was not changed when the layers were piled up. The reason for this is that the spherical shape was barely formed due either to the small amount of PAAS or the size of these PAAS particles being too small. A small particle size cannot influence the multilayer inner structure. On the other hand, spherical shape particles were observed in the case of LF 43. As shown in Figure 5, the second layer covered by PAAS showed the aggregation of PAAS particles. No particle aggregation was observed in the third layer covered by PMDA-ODA PI. The next layer contains uniform sized particles. This means that the electrostatic interaction between layers can lead to the crystallization of PAAS particles. The particle size was 20~40 nm. In the case of LF21 (Figure 6), some particles showed layers with ammonium salts. However the ordering was not good. Too much salt might obstruct the interaction between the polymer chains and cause phase separation. These irregular particles disturb multilayer film formation, which results in a poorer domain morphology. In the case of LF21, which had low molecular weight, the chains were too short to form a sphere, leading to the irregular growth of particles. These irregular particles appear to become a disturbance factor for the interactions between each polyimide layer.

The particle size was also obtained using dynamic light scattering measurements (Figure 7). The particle size of the three samples ranged from 11 to 27 nm (Table II). Spherical shaped particles were formed. The particle sizes of the three samples with different molecular weights were similar. This

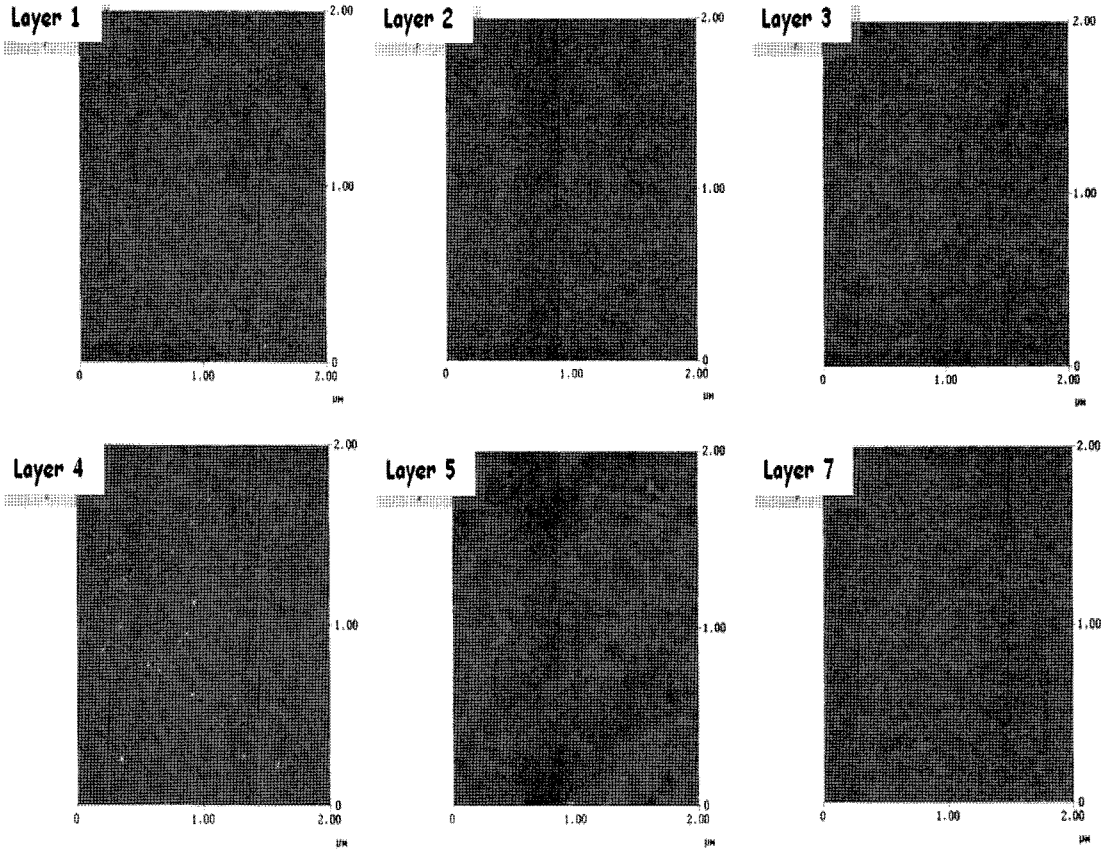

Figure 4. AFM images of LF11 polyimide multilayer thin films with different numbers of layers.

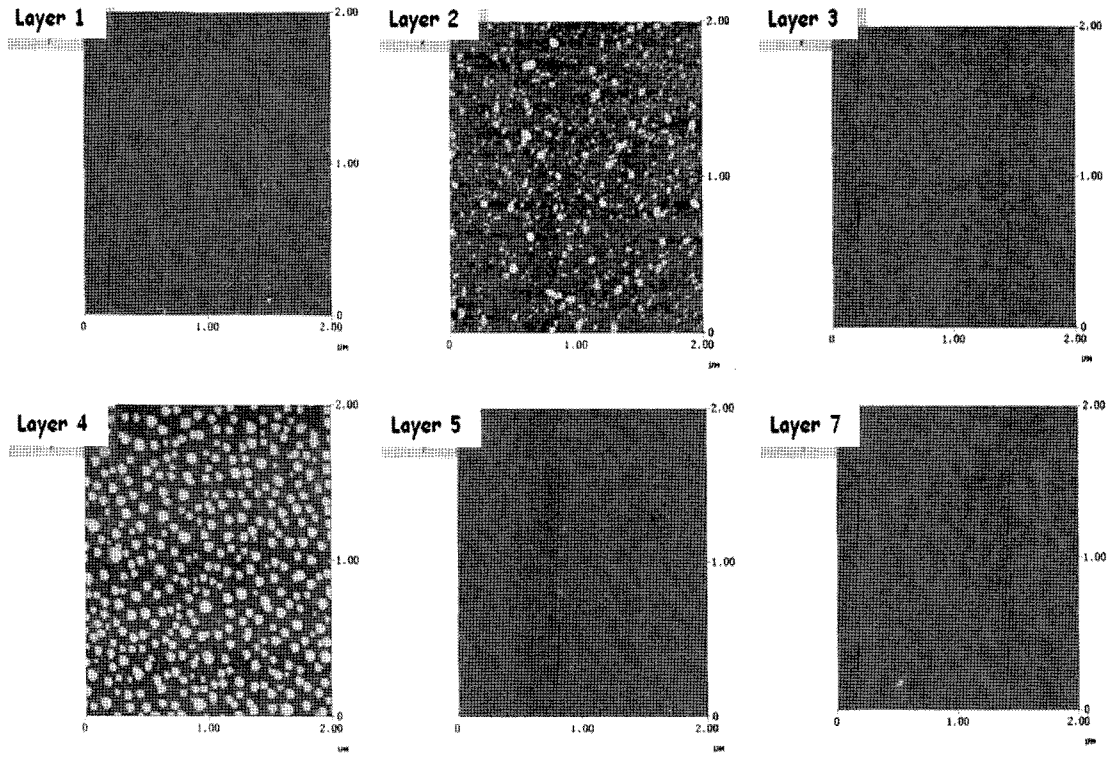

Figure 5. AFM images of LF43 polyimide multilayer thin films with different numbers of layers.

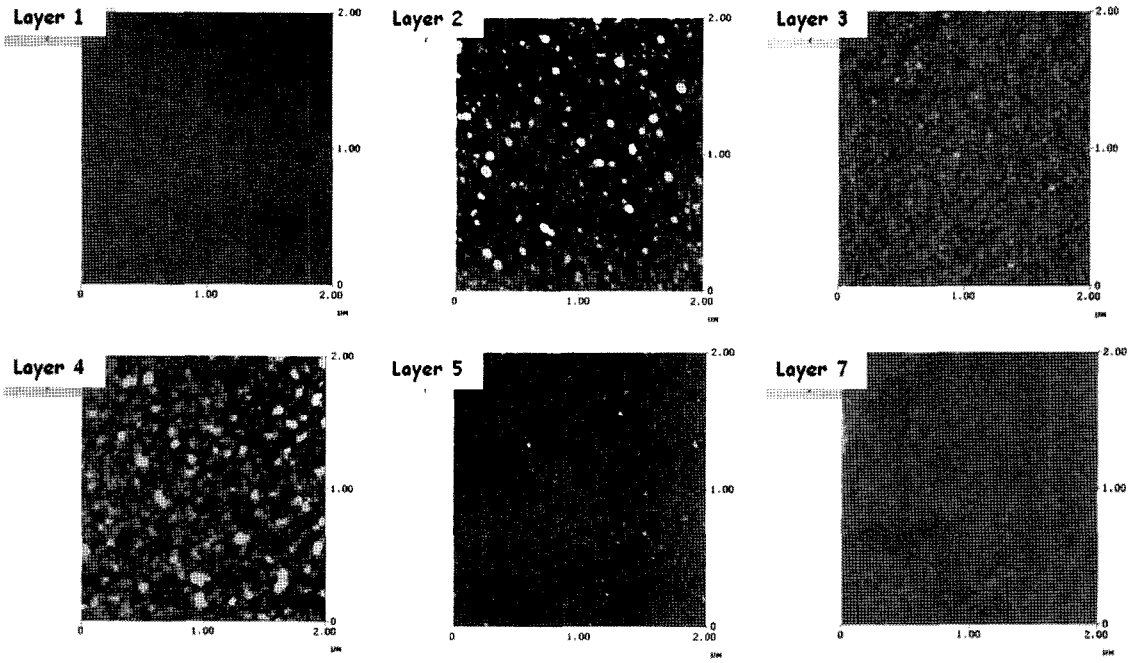

Figure 6. AFM images of LF21 polyimide multilayer thin films with different numbers of layers.

Table II. Particle Size of LF11, LF43, LF21 by Dynamic Light Scattering

Sample Name	Particle Size (nm)	Standard Deviation
LF11	11	0.006
LF43	11	0.002
LF21	27	0.010

means that the particle size is not influenced by the chain length. The data is in agreement with the AFM images. As shown in Table II, the standard deviation of LF11, LF43, and LF21 was 0.006, 0.002 and 0.01, respectively. These values mean that almost uniform sized particles exist in a solvent. This data is in accordance with the lower polydispersity observed in the GPC data. It should be noted from those AFM images, however, that the spherical aggregates between layers hint inherent immiscibility of PAA and PAAS.

X-ray Analysis. Small-angle X-ray reflectance (XRR) was also used to examine the film structure. Figure 8 shows the XRR curves for the PI multilayer thin films. Samples with 7 layers were deposited on a Si-wafer. A broad oscillation was observed after 0.3° in each XRR curve of the multilayer thin films, which is considered to be a Kiessig fringe.[16-19]

Table III. Thickness of Polyimide Multilayer Films by α-Step

Sample Name	Thickness (Å)
LF11	6,100
LF43	5,900
LF21	6,300

The film thickness can be obtained from the Kiessig fringe using the reflectance angle θ as a unit of measure. The ΔQ_z value was derived from the equation, $Q_z(\text{Å}^{-1})=4\pi \sin \theta/\lambda$, where λ (1.541 Å) is the wavelength of Cu-K_α radiation used in the XRR experiment. ΔQ_z was found to be approximately 0.0010 Å^{-1} for LF 11, which corresponds to a total film thickness ($d_{total}=[2\pi/\Delta Q_z]$) of 6,280 Å. This value agrees well with the overall thicknesses determined by α-step (6,300 Å) (Table III). In addition, two peaks were observed at around 0.3° (2θ) and 0.4° (2θ), respectively. In the case of LF11, the calculated values of the two peaks were 284 Å and 220 Å, respectively, meaning there is a gap between the two layers. These peaks may be formed by the difference in height due to the centrifugal force during spin-coating. In the case of LF 43, the values were 274 Å and 213 Å, respectively. The d-spacing was decreased by the inserted ammonium salts, because the ordered PAAS particles increased the interaction of the interface. Since both the cationic and anionic moieties of the PAAS increases on increasing the amount of ammonium salt, the intermolecular interaction between PAAS becomes stronger, so as to enhance dewetting nature of PAAS onto PAA layer. However, in the case of LF21, the value was increased due to the irregularity of the PAAS particles. Effects of such intermolecular interaction on the crystallization behavior of the multilayer systems, if any, are under investigation using X-ray diffraction and differential scanning calorimeter, etc. and will be reported elsewhere.

Optical Properties. A 7 layers film was deposited on a silicon wafer to allow UV-Vis spectroscopy. Figures 9, 10 and 11 show the UV-Vis spectra of the LF11, LF43 and

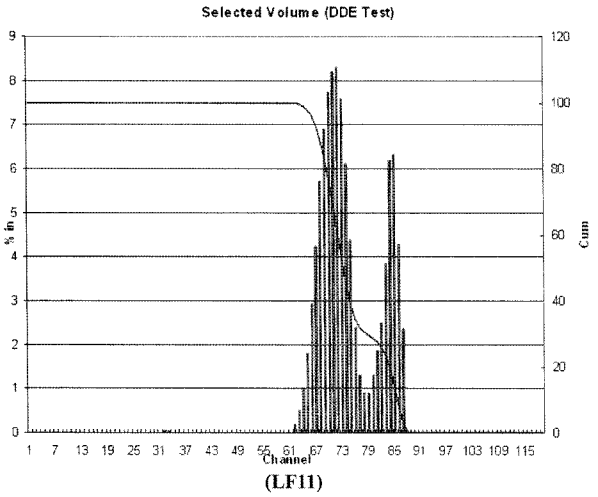

(LF11)

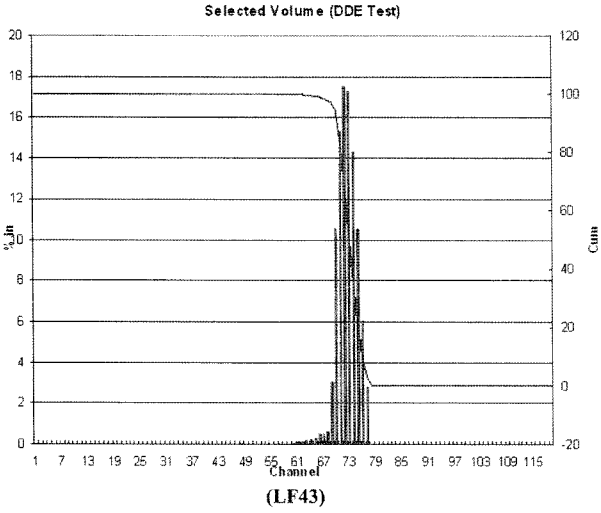

(LF43)

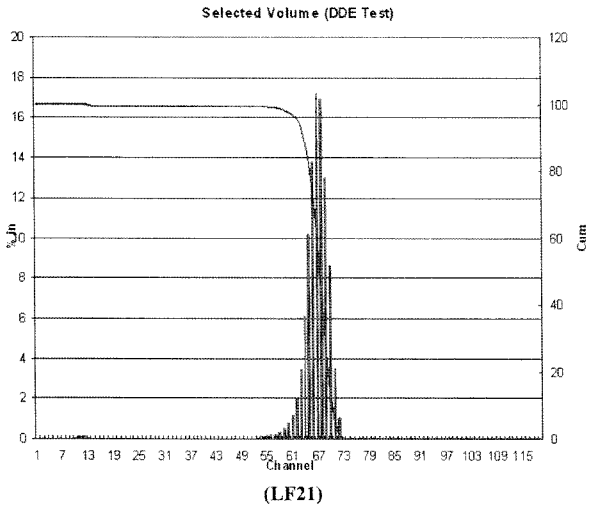

(LF21)

Figure 7. The particle size distribution of LF 11, LF 43 and LF21 by dynamic light scattering.

LF21 multilayers, respectively. A larger number of molecules can absorb light of a given wavelength, which means more light can be absorbed. Furthermore, the extent of light

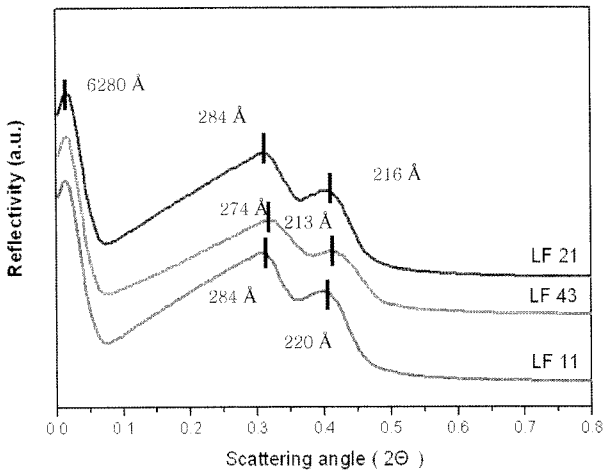

Figure 8. X-ray reflection curves of polyimide multilayer thin films of LF11, FL43 and LF21.

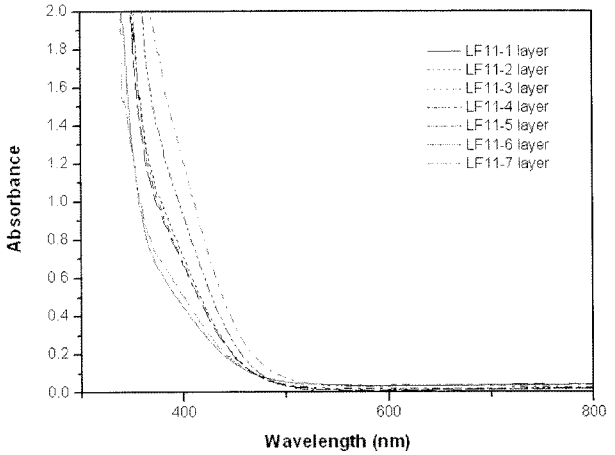

Figure 9. UV-Vis spectra of LF11 polyimide multilayer thin films with different numbers of layers.

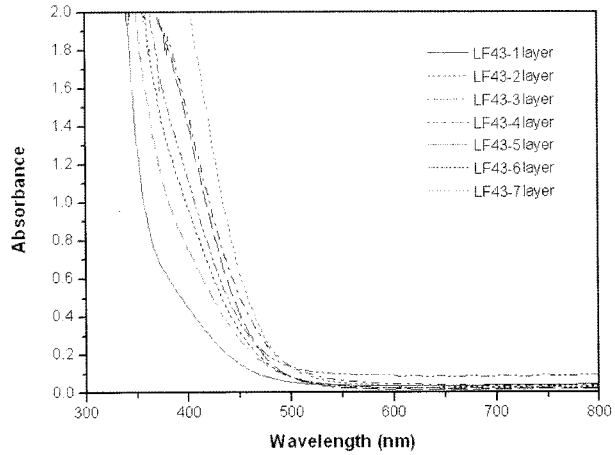

Figure 10. UV-Vis spectra of LF43 polyimide multilayer thin films with different numbers of layers.

absorption increases as the molecules absorb light of a given wavelength more effectively. From this, the following

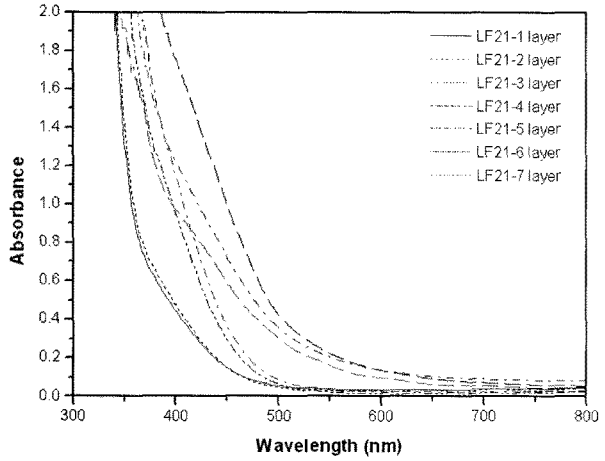

Figure 11. UV-Vis spectra of LF21 polyimide multilayer thin films with different numbers of layers.

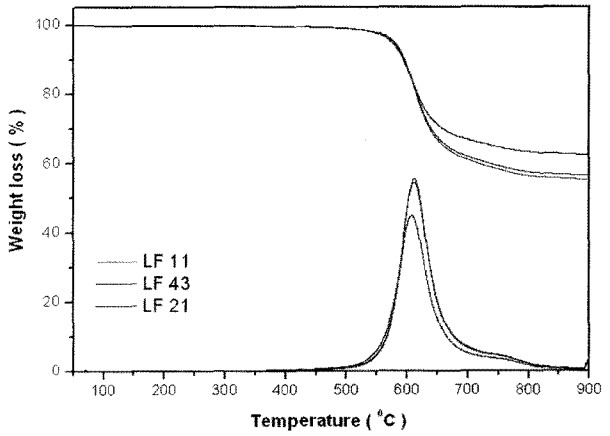

Figure 12. TGA and DTG curves of polyimide multilayer thin films.

empirical expression, known as the Beer-Lambert law,[20] was formulated.

$$A = \log 10 (I_0/I)$$

where A is the absorbance, I_o is the intensity of light incident upon a sample cell, and I is the intensity of light leaving sample cell. The absorbance, A, has a linear relationship with the length of a sample cell, i.e. the number of layers deposited. Therefore, a linear increase in the maximum absorption intensity in the UV-Vis spectra of multilayer thin films shows that the deposition of a layer on a substrate is well controlled. Figure 9 shows the UV-Vis spectra of a LF11 film with 7 layers on a silicon wafer. Here, the edge of the absorbance wavelength was shifted to a longer wavelength with increasing the number of layers. However, there was no change between layers 3 and 5. This means that small amount of salt does not affect on the optical properties in the case of LF11. However, in the case of LF 43 (Figure 10), the absorption followed the Beer-Lambert law. LF21 (Figure 11) showed a somewhat different trend. For the second layer, the absorption edge was shifted to the right and the absorbance was higher than with the first layer. This means increased aggregation of salts between the chains. For the third layer, the absorption edge was shifted to the left and the absorbance intensity was lower than that of the second layer. These trends are repeated as another layer was added.

Thermal Stability. Figure 12 shows the TGA and differential thermogravimetric (DTG) curves of the PI multilayer thin films. The average decomposition temperature was 611 °C. All the films show an almost single step thermal decomposition behavior. As the AFM images showed the existence of particles, the TGA curves provided evidence that the PAAS particles did not decompose until the imide chains had decomposed. This means that the PAAS layers protected the polyimide layers because it exists between two polyimide layers.

Conclusions

PI multilayer thin films were prepared by spin coating. Pyromellitic dianhydride (PMDA)-4,4′-oxydianiline (ODA) polyimide was prepared, and PAAS was obtained by incorporating triethylamine (TEA) into PMDA-ODA poly(amic acid) (PAA) in dimethylacetamide. Different PAAS were prepared with different compositions. The FT-IR and ^{1}H NMR spectra of the polyimide multilayer thin films confirmed the imidization of PAA. The nanostructure of the multilayer thin films was confirmed by XRR. LF 43, which is in an oligomer state, has a uniform spherical shape of PAAS particles. The uniform particles influenced the nanostructure of the interlayer by increasing the interaction forces, which is supported by AFM results. UV-Vis spectroscopy showed that the LF 43 multilayer followed the Beer-Lambert law. It was found that the relationship between the uniformity of the PAAS particle shapes and the interaction between layers affects the optical and thermal properties of PI layered films.

Acknowledgements. This work was supported by a grant from the Fundamental R&D Program for Core Technology of Materials funded by the Ministry of Knowledge Economy, Republic of Korea, the Korea Science and Engineering Foundation (KOSEF) through the National Research Laboratory Program funded by the Ministry of Education, Science and Technology (MEST; M10300000369-06J0000-36910), the SRC/ERC Program of MEST/KOSEF (grant # R11-2000-070-080020), the Brain Korea 21 Project, and the Korea Electrotechnology Research Institute.

References

(1) P. K. Ho, J. S. Kim, J. H. Burroughes, H. L. Becker, T. M. Brown, F. Cacialli, and R. H. Friend, *Nature*, **404**, 481 (2000).
(2) X. Zhang and J. Shen, *Adv. Mater.*, **11**, 1139 (1999).
(3) J. D. Mendelson, C. J. Barrett, V. V. Chan, A. J. Pal, A. M. Mayes, and M. F. Rubner, *Langmuir*, **16**, 5017 (2000).

(4) A. Laschewsky, E. Wischerhoff, M. Kauranen, and A. Persoons, *Macromolecules*, **30**, 8304 (1997).
(5) Y. He, S. Gong, R. Hattori, and J. Kanicki, *Appl. Phys. Lett.*, **74**, 2265 (1999).
(6) B. S. Kim, S. H. Bae, and Y. H. Park, *Macromol. Res.*, **15**, 357 (2007).
(7) J. Y. Lee, J. H. Kim, and B. K. Rhee, *Macromol. Res.*, **15**, 234 (2007).
(8) H. S. Lee, A. Roy, and A. S. Badami, *Macromol. Res.*, **15**, 160 (2007).
(9) A. S. Mathews, I. Kim, and C. S. Ha, *Macromol. Res.*, **15**, 114 (2007).
(10) K. Sato, S. Harada, A. Saiki, T. Kimura, T. Okubo, and K. Mukai, *IEEE Trans.*, **9**, 176 (1973).
(11) J. D. Rancourt and L. T. Taylor, *Macromolecules*, **20**, 790 (1987).
(12) Y. Ding, B. Bikson, and J. K. Nelson, EPA Patent 1,086,737 (2001).
(13) C. Morris and A. Barry, *J. Plastic Film & Sheeting*, **23**, 97 (2007).
(14) P. A. Chiralli, *Langmuir*, **18**, 168 (2002).
(15) J. A. Kreuz, A. I. Endrey, F. P. Gay, and C. E. Sroog, *J. Polym. Sci. Part A: Polym. Chem.*, **4**, 2607 (1966).
(16) M. Scaub, C. Fakirov, A. Schmidt, G. Lieser, G. Wenz, G. Wegner, P. A. Albouy, H. Wu, M. D. Foster, C. Majrkzak, and D. S. Satija, *Macromolecules*, **28**, 1221 (1995).
(17) I. C. Kjaerm, J. Als-Nielsen, C. A. Helm, P. Tippmann-Krayer, and H. Mohwald, *Thin Solid Films*, **159**, 17 (1988).
(18) F. Rieutord, J. J. Benattar, R. Rivoira, Y. Lepbtre, C. Blot, and D. Luzet, *Acta Crystallogr.*, **A45**, 445 (1989).
(19) T. P. Russell, *Mater. Sci. Rep.*, **5**, 171 (1999).
(20) D. L. Pavia, G. M. Lampaman, and G. S. Kriz, *Spectroscopic Methods in Organic Chemistry*, Harcourt College Publishers, USA, New York, 2001, p. 279.